Preparation and Characterization of Magnetite Nanoparticle and Biochar from Unripe Banana Peels from Biara in River State, Nigeria

[1]Ideriah T. J. K., [2]Ighomuaye, M. N., [3]Boisa N., [4]Cookey G. A.

[1]**Institute Of Pollution Studies, Rivers State University Nkpolu Oroworukwo, Port Harcourt**

[2,3,4]**Department Of Chemistry, Rivers State University Nkpolu Oroworukwo, Port Harcourt**

ABSTRACT

In this study magnetite nanoparticle and biochar (adsorbents) were produced and characterized using Scanning Electron Microscopy (SEM), Transmission Electron Microscopy (TEM), X-Ray diffraction (XRD) and Fourier Transform Infrared Spectrometer (FTIR). Results from FTIR revealed the presence of OH functional group which enhanced absorption. TEM micrograph of the biochars were agglomerated and spherical while magnetite nanoparticles were agglomerated, partially spherical, cubic shape and have an amorphous structure at 50 nm with the inclusion of its properties aids absorption of pollutants. SEM morphology of the surface adsorbent have pores, cracks, holes which are expected to enhance adsorption at 10 nm in a higher magnification (2000 X). The SEM images of the iron size nanoparticle had a rod shape morphology and also were agglomerated due to its magnetic properties which matched with EDS and XRD data. The shape of the nanoparticles prepared by decantation differs from those prepared from filtration. The XRD Powder for the adsorbents were similar to that of graphite. The peaks denote the formation of a crystalline carbonaceous structure. The average particle size of the adsorbents at 11 nm confirmed that the synthesized nanoparticles were nanocrystalline in nature. Therefore, these adsorbents are recommended for the remediation of polluted soils due to their properties which will enhanced absorption

Keywords: Magnetite Nanoparticle, Biochar, Pyrolysis, Absorption, Banana, Peels

INTRODUCTION

Recently, worldwide there has been an adverse impact on the environment due to man's total involvement in anthropogenic activities for economic development. Soil is one of the components of the environment that is severely affected by various anthropogenic activities. [1], reviewed that about 77 % of oil spilled from 1976 to 1996 were not recovered thereby reducing soil fertility which lead to destruction of soil microbes, groundwater pollution, alteration of geological properties of the impacted soil, poisoning of sea foods and other aquactic habitats [2]. This will then call for a positive ways of handling these problems in other to make the ecosystem conducive for its inhabitants. Nanoparticles are particles ranging 1-100nm [3]. Nanoparticles could be loosed or agglomerated [4]. Nanoparticles could be uniform, or made of different layers.

Magnetite nanoparticle (Fe_3O_4) is an iron oxide, which have an inverse spinel structure. Magnetite nanoparticles (Fe_3O_4) have various applications due to their specific magnetic properties such as high surface area, and unique dimensions. The chemical composition of MNPs are of various types namely; pure metals, alloys, metal oxides, and doped MNPs. MNPs could be coated and functionalized according to the user's needs.

Biochar is a carbon-rich product produced from pyrolysis at high temperature (300–900 °C) of carbonaceous biomass in a closed system [5] and [6]. Agricultural materials that have been studied as biochar are yam peels, wheat straw, sawdust, plantain, acacia, gliricidia, oil palm bunch, rice residues, corncob, coconut husk, kenaf

fibre, kapok fibre, cotton, wool, and wood [7]. Benefits of using these materials include they are cheaper, biodegradability, and non-toxic [8]. These unique properties of magnetite nanoparticle and biochar will make them the most efficient tool for environmental remediations [9].

MATERIALS AND METHODS

The Study Area

Biara (as the crow flies) is a town in Gokana Local Government Area of Rivers State in the South-South geopolitical zone of Nigeria. It is located in the Northeast region of Gokana on latitude 519781 and longitude 308886. Biara is 34 km / 21 mi away from Rivers State Capital, Port Harcourt. It is situated between Bela and Nwabia communities. The People of Biara speak Gokana language. Biara people are traditionally farmers; farming a variety of crops such as plantain, oil palm, cassava, okra, melon, and banana, fishermen; making of fishing nets, construction of canoes and traders. Biara is a community bless with crude oil but due to anthropogenic activities, oil have released contaminants thereby causing reduction in farmland fertility and aquactic organisms. Their climate is tropical.

Preparation of Magnetite Nanoparticle

The magnetite nanoparticle was prepared using the modified method of [10]. The iron (II) and iron (III) solutions were prepared by dissolving 4.40 g of $FeCl_2.4H_2O$ and 1.98 g of $FeCl_3.6H_2O$ in 60.0 mL of deionized water. The mixture was stirred thoroughly and then reacted with 0.44 M NaOH droplets until the solution turned blackish with continuous stirring. 168.0 mL of NaOH was used before the black magnetite precipitates was formed. The black precipitate was separated by placing a bar magnet by the side of the test tube while decanting the clear supernatant then precipitates were divided into two, filtered and decanted, washed with ethanol The magnetite precipitates were dried at 80 ^{o}C in an oven overnight and stored in capped sample bottles. The extract characterized using Scanning Electron Microscopy (SEM), Transmission Electron Microscopy (TEM), X-Ray diffraction (XRD), Fourier Transform Infrared Spectrometer (FTIR) and Atomic Absorption Spectrophotometer (AAS).

Preparation and Characterization of Unripe Banana Biochar

Biochar were produced from Gros Michel and Cavendish unripe banana peels using modified method of [11]. Biochar were produced from unripe banana peel. The banana was purchased from a mami market, Rainbow Town in Rivers State, washed thoroughly under a running water to remove dirt's, peeled and cut into small sizes and dried under the sun five days. The sun-dried banana peels was crushed to increase the surface area, sieved through 100- μm mesh. Biochar were produced by the pyrolysis of the sun dried unripe banana samples in a muffle furnace having an oven on top and release volatile gas within at 500°C in the absence of air for three hours and allow to cool, the charcoals were removed from the crucible, sieved, and stored in an air- tight container. SEM, TEM, XRD, FTIR and AAS analysis were carried out to determine its average pore width, micropore volume, micropore surface area and their metal concentrations.

RESULTS

### Characterization of magnetite nanoparticle and biochar

The analyses of magnetite nanoparticle and biochar are presented in Tables 1 –3**.**

FTIR Study

FTIR spectrum of various synthesized adsorbents are shown in figures 1a (I) – 1a (IV). Peaks and frequencies of IR absorption are presented in Table 1. The adsorbents peak ranges were 701 cm^{-1} to 3131 cm^{-1} in Cavendish biochar, 1059 cm^{-1} to 2684 cm^{-1} in decanted magnetite nanoparticle, 850 cm^{-1} to 2654 cm^{-1} in filtered magnetite nanoparticle and 753 cm^{-1} to 3019 cm^{-1} in Gros Michel biochar.

Table 1: Peaks and Frequencies of IR Absorption by the Studied Adsorbents

Peak (cm^{-1})				
Cavendish Biochar	Fe$_3$o$_4$ Decanted	Fe$_3$O$_4$ Filtered	Gros Michel Biochar	Functional Group Assignment
701			753	
872		850	850	C-Cl stretch due to alkyl halide
1036	1059		1044	C-H ''oop''
1379	1320	1320	1379	C–O–H stretch
1446				C-H rock
1566	1513	1506	1566	NO$_2$ symmetric stretch due to nitro compound
	1774			-C=C stretching
2341	2341	2341	2341	C-H bend due to alkanes
	2684	2654		-C≡C- stretch
3131			3019	O–H stretching
				OH stretch
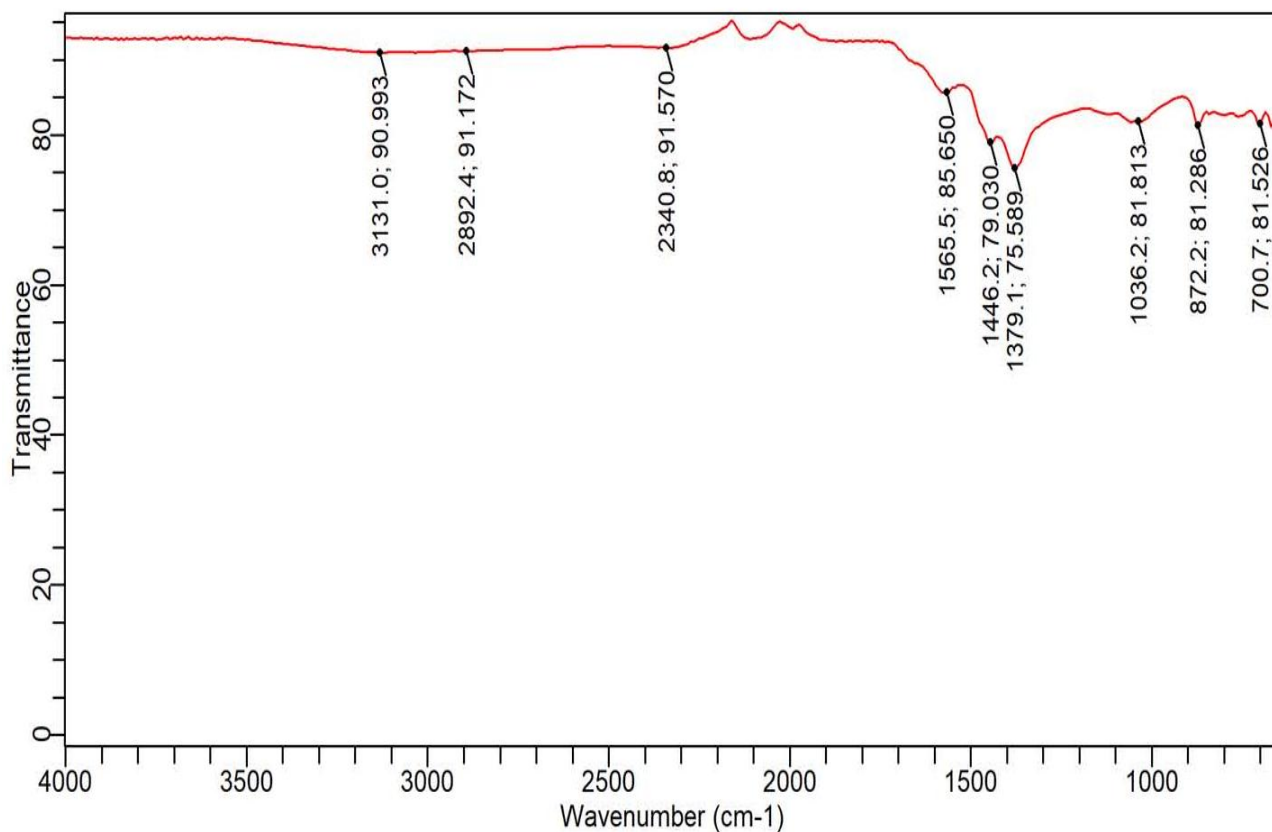
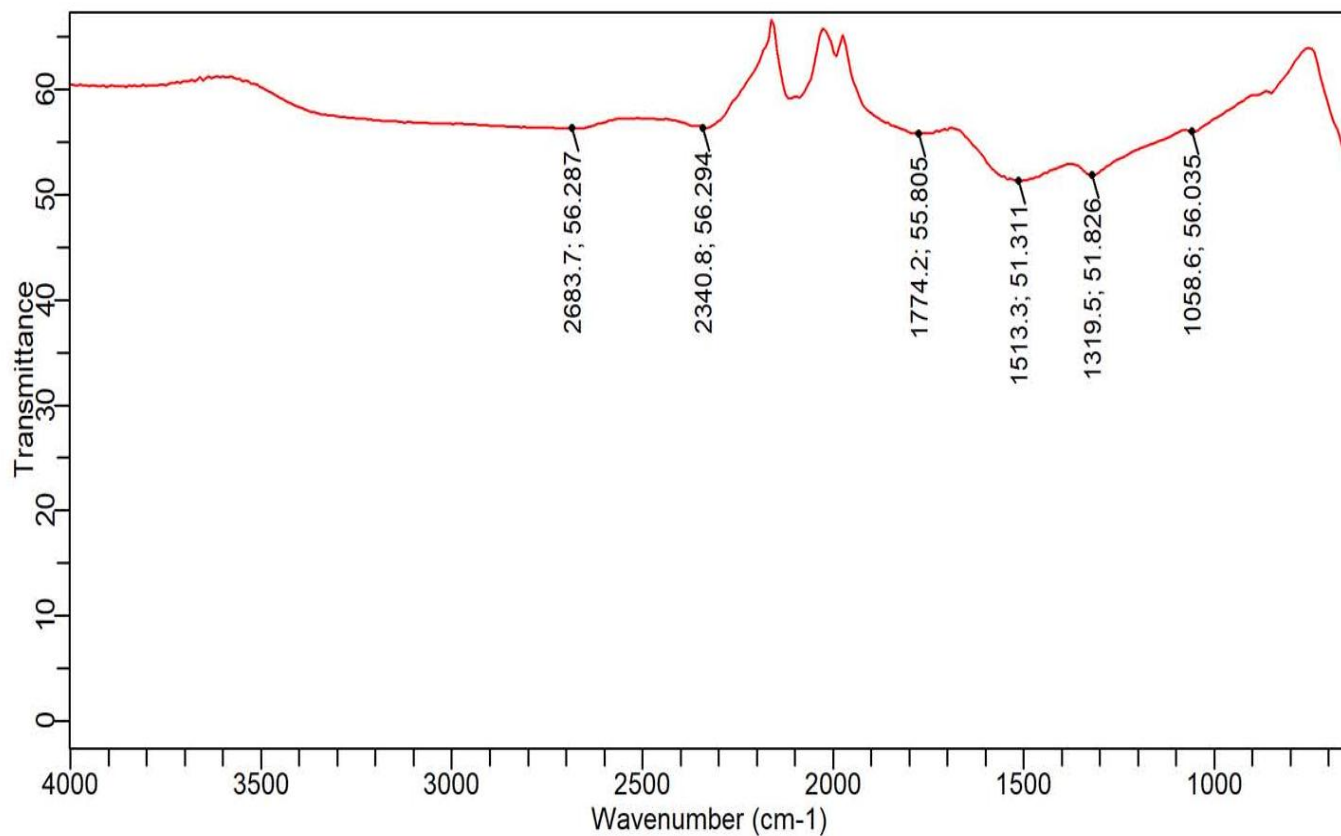**Figure 1a (I): FTIR of Cavendish Biochar**

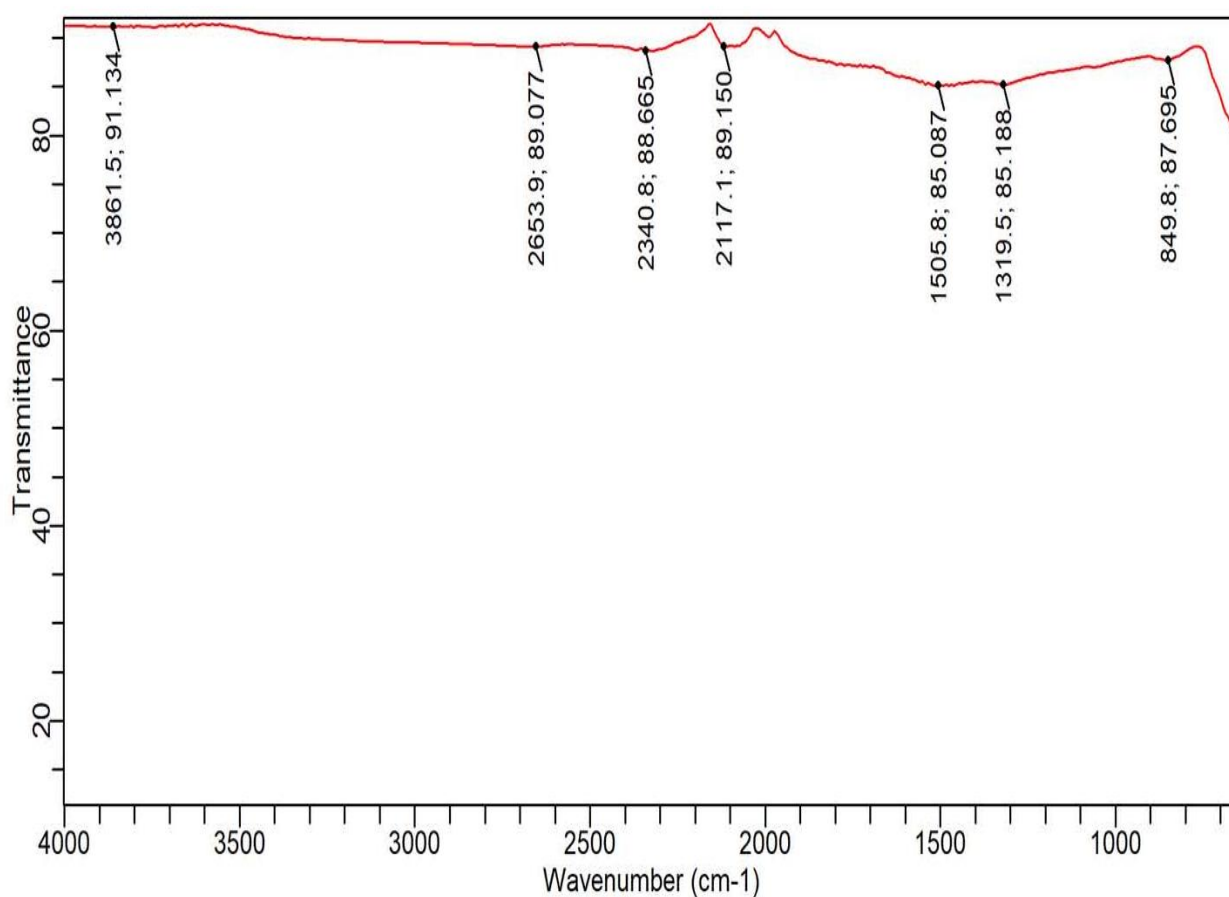**Figure 1a (II): FTIR of decanted Fe₃O₄**

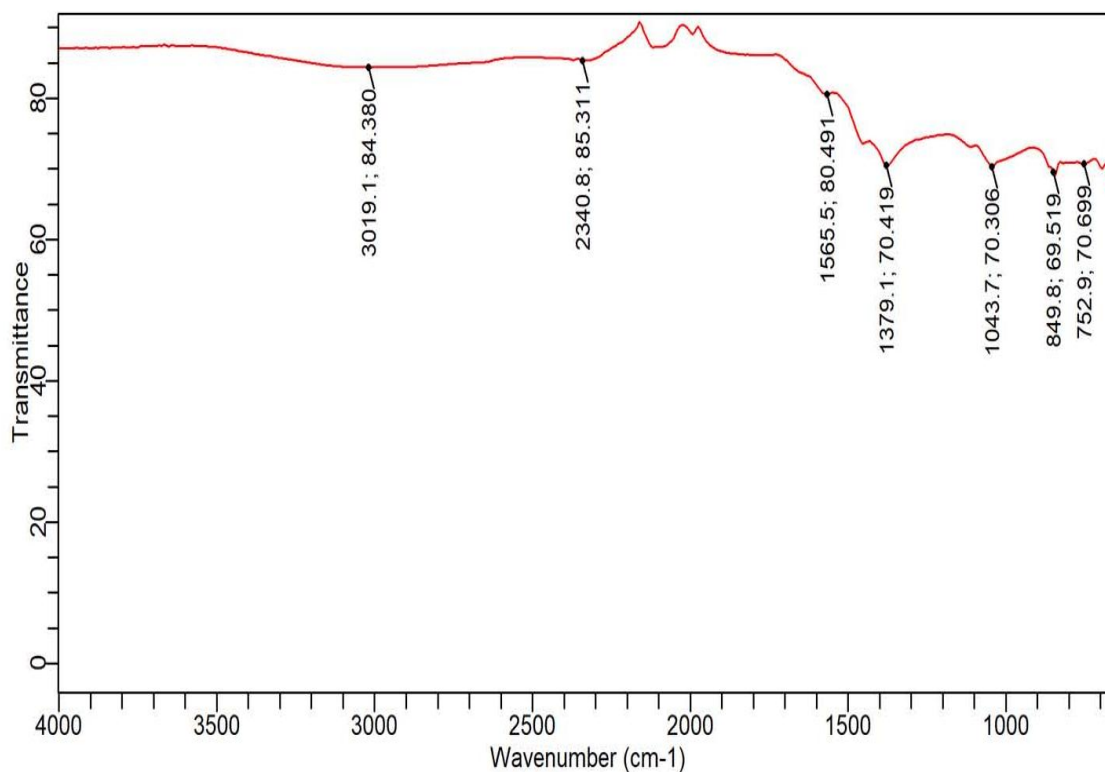**Figure 1a (III): FTIR of Filtered Fe₃O₄**

Figure 1a (IV): FTIR Gros Michel Biochar

TEM Analysis

TEM morphology of synthesized adsorbents (Gros Michel Biochar, Cavendish Biochar, Decanted Fe_3O_4 and Filtered Fe_3O_4) are displayed in figure 1b (I) for Gros Michel Biochar, Cavendish Biochar 1b (II), decanted iron oxide nanoparticles 1b (III) and figure 1b (IV) for filtered iron oxide nanoparticles.
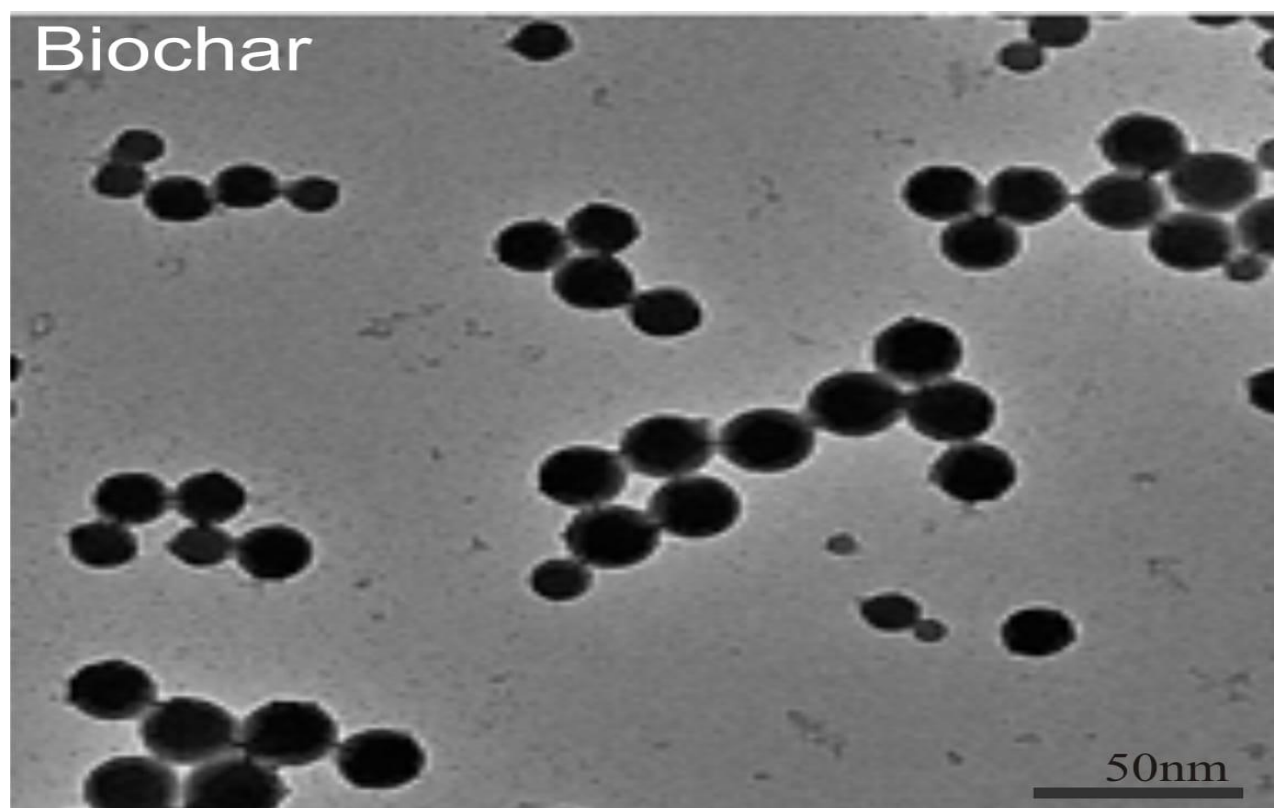

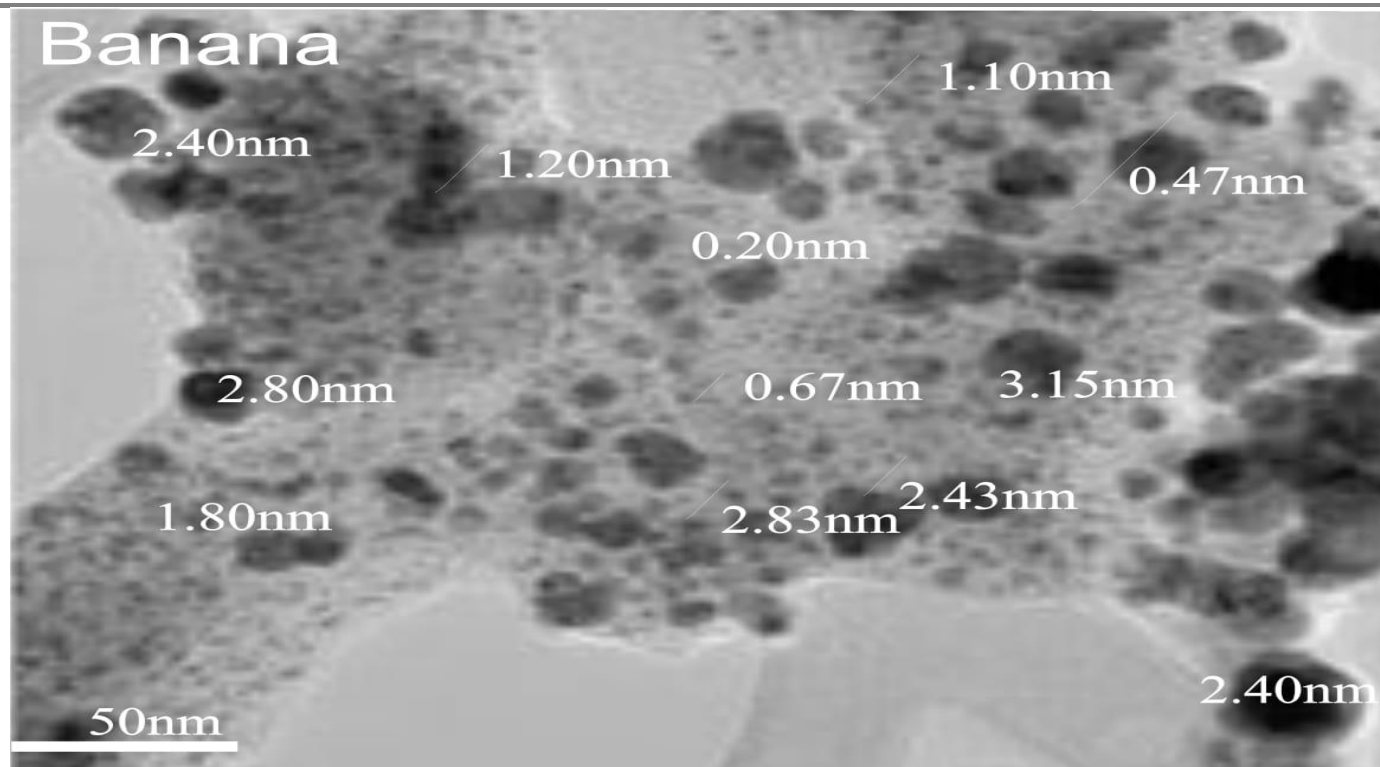**Figure 1b (I): TEM image of Gros Michel Biochar**

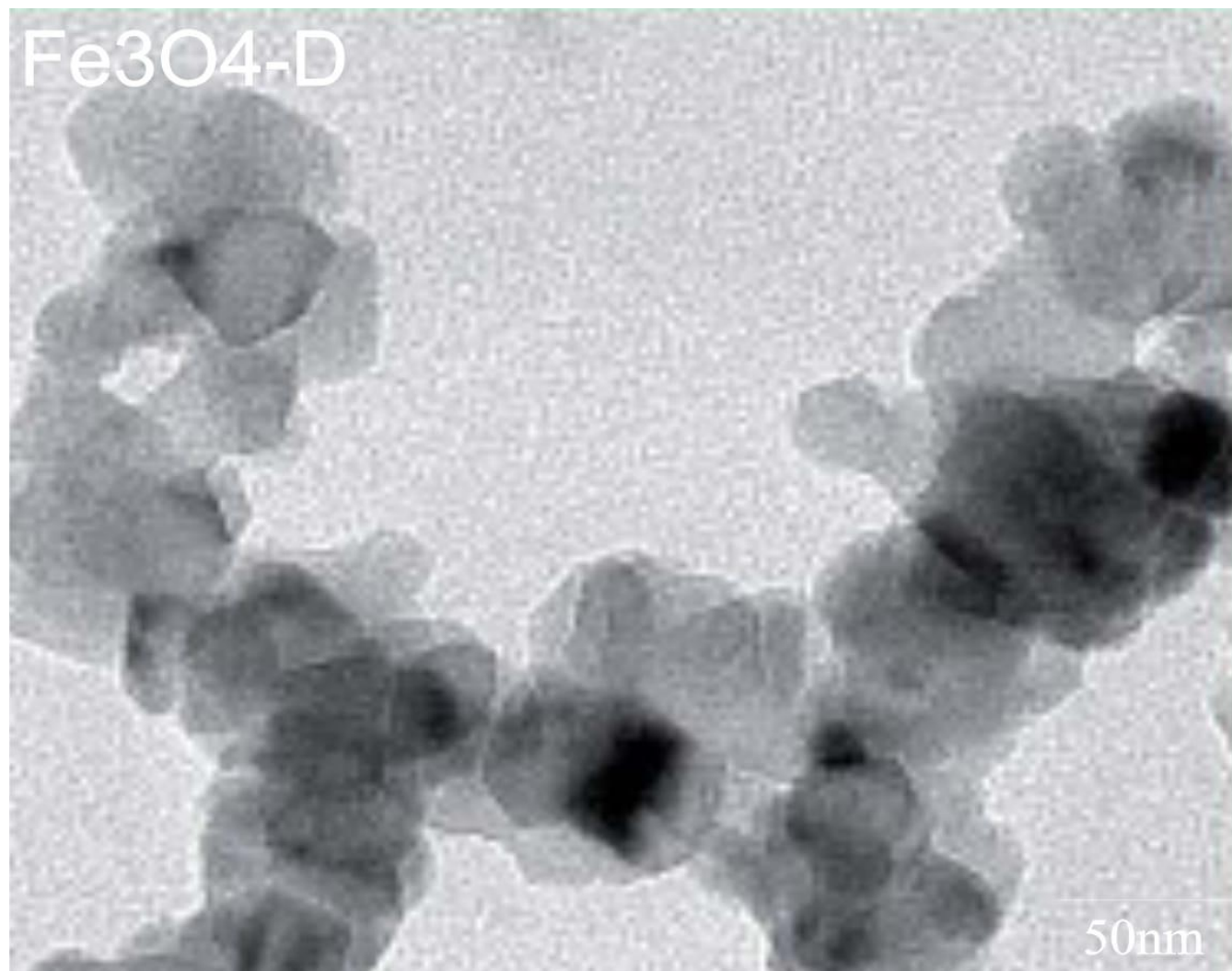**Figure 1b (II): TEM image of Cavendish Biochar**

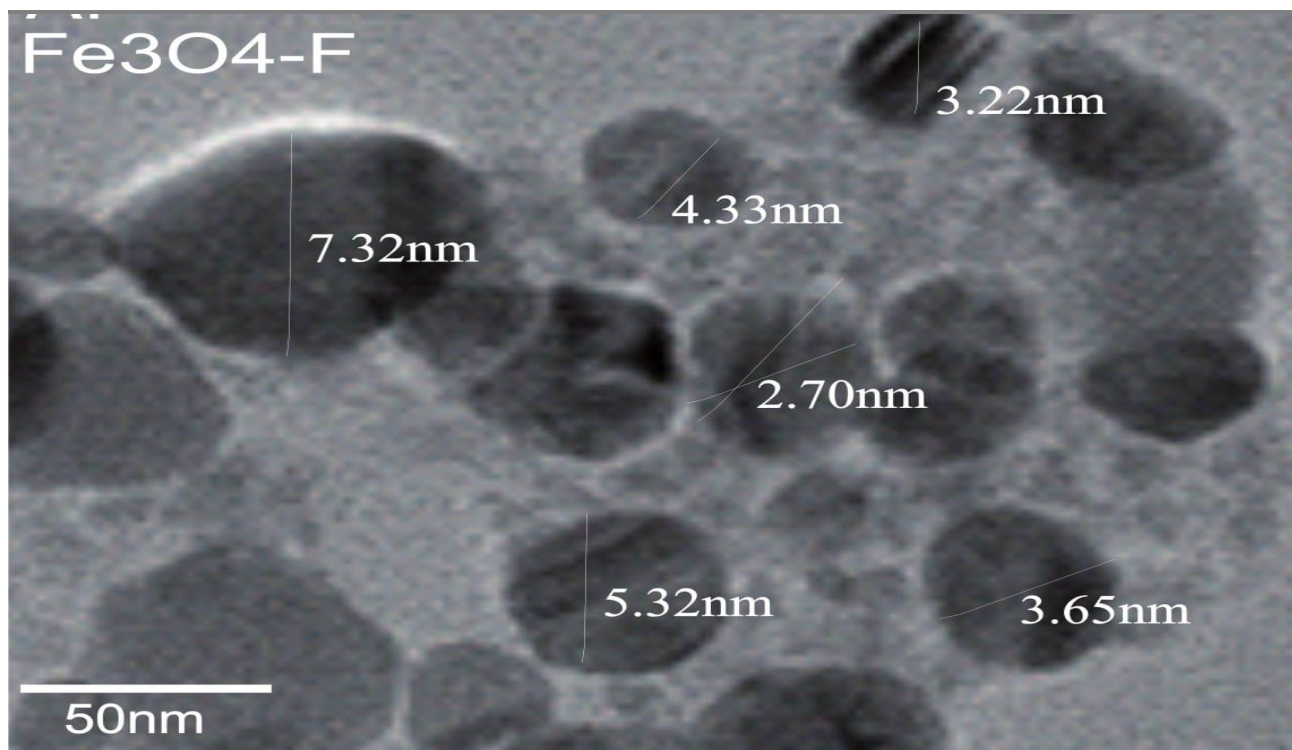**Figure 1b (III): TEM image of Fe₃O₄ Decanted**

Figure 1b (IV): TEM image of Fe₃O₄ Filtered

SEM and EDX Analysis

SEM surface morphology of adsorbents Gros Michel Biochar, Cavendish Biochar, Fe_3O_4 D and Fe_3O_4 F at 10 µm are shown in figures 1c (I) - 1c (IV). EDX spectra peaks and elements of adsorbents Gros Michel Biochar, Cavendish Biochar, Fe_3O_4 D and Fe_3O_4 F are displayed in figures 1c (V) - 1c (VIII) and Table 2.
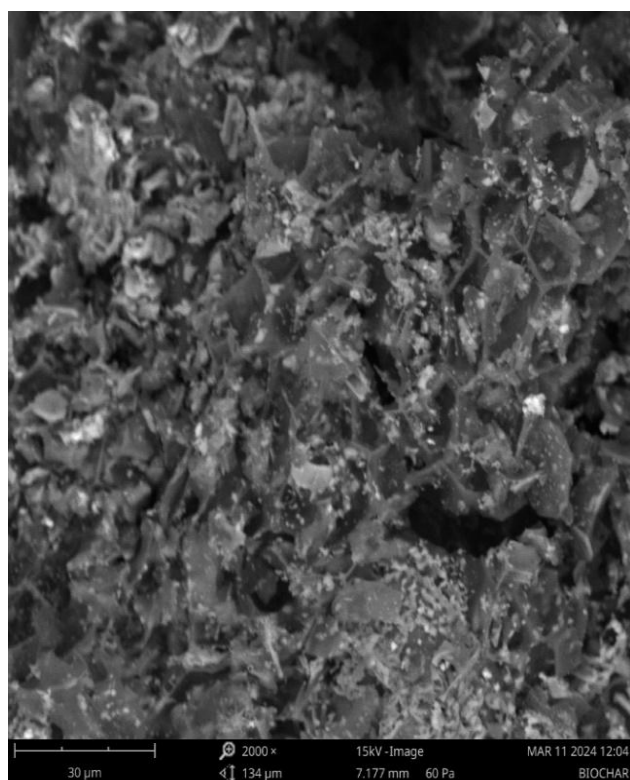
(A)
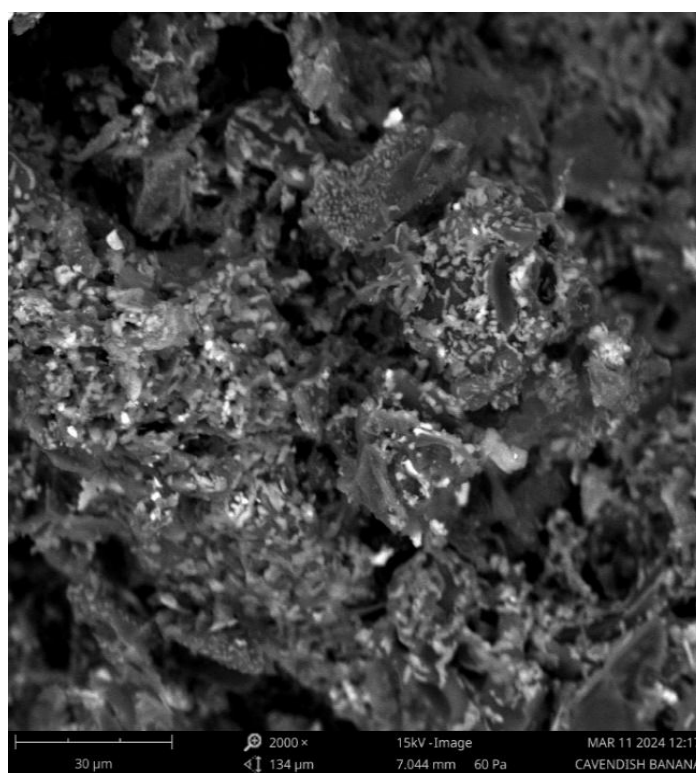
(B)

Figure 1c (I) SEM images of Gros Michel Biochar at 10 µm scale and a magnification of 2000 X

Figure 1c (II) SEM images of Canvendish Biochar
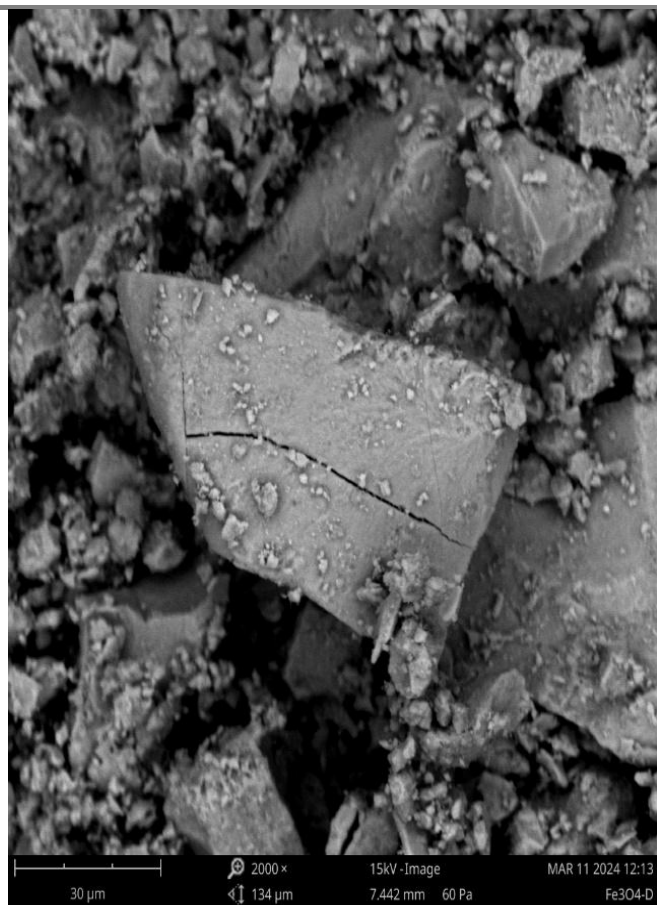
(C)
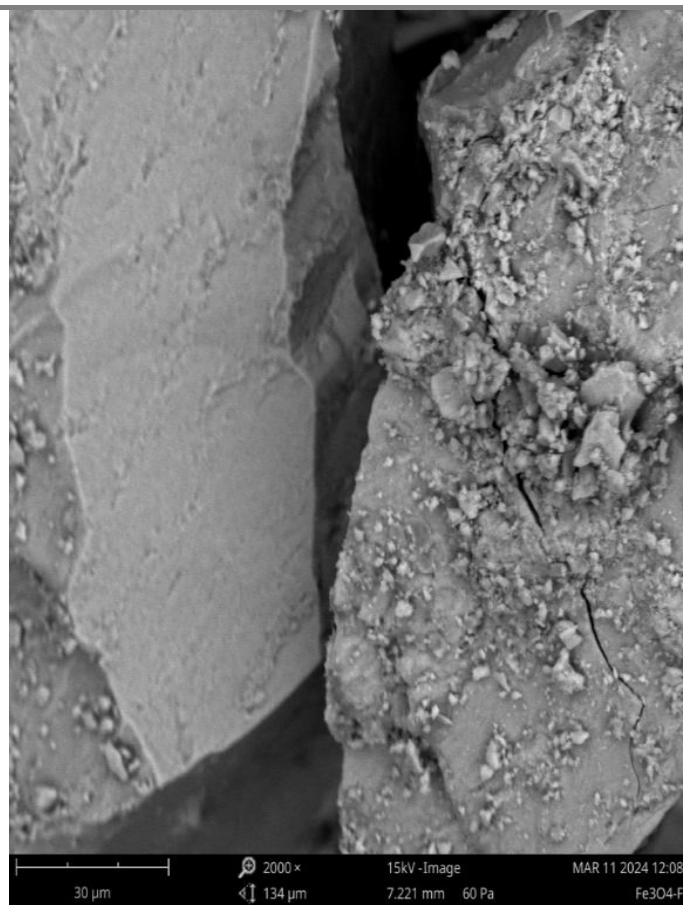
(D)

Figure 1c (III) SEM images of D Fe₃O₄ **Figure 1c (IV) SEM images of F Fe₃O₄**
at 10μm scale and a magnification of 2000 X
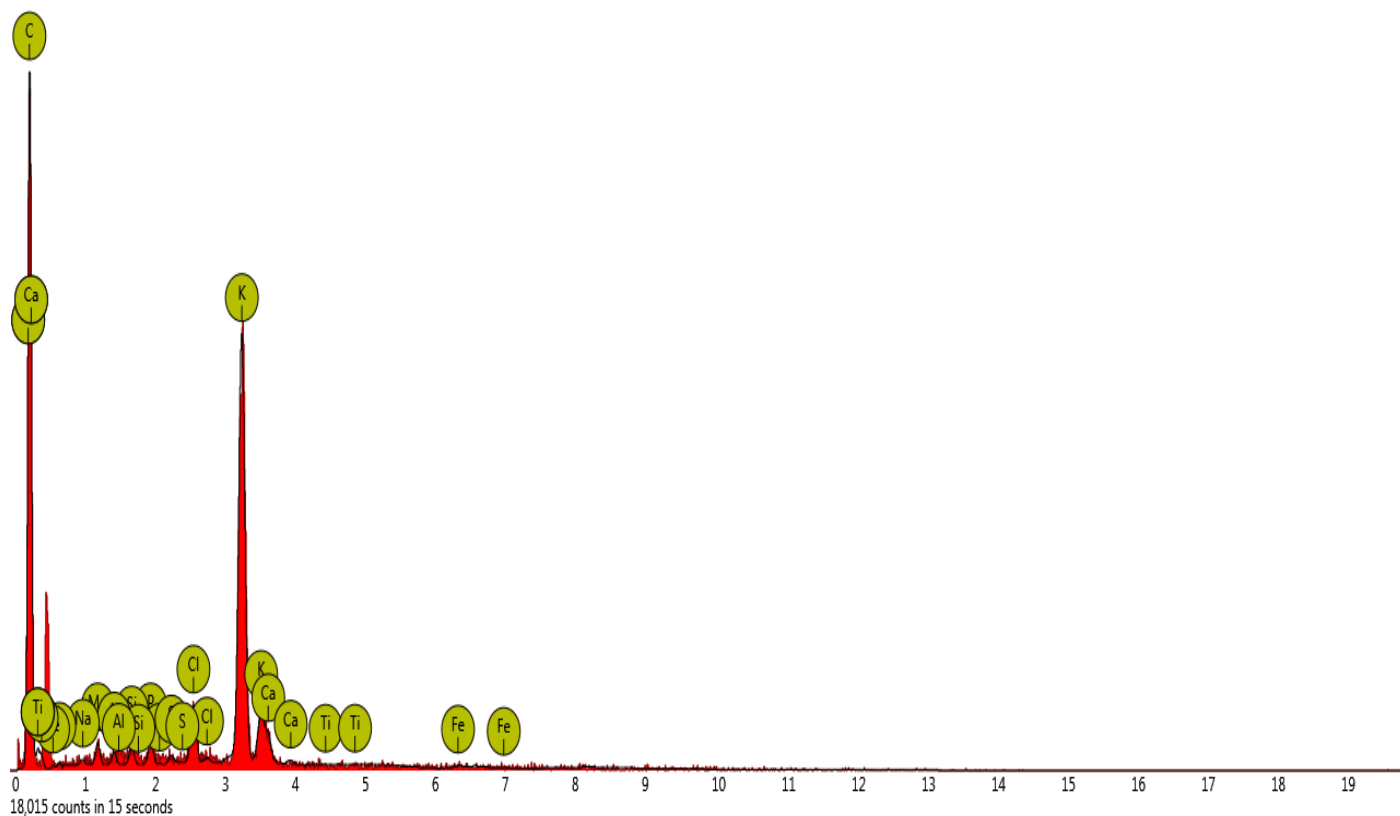
(E) Figure 1c (V): Elemental analysis of Cavendish Biochar
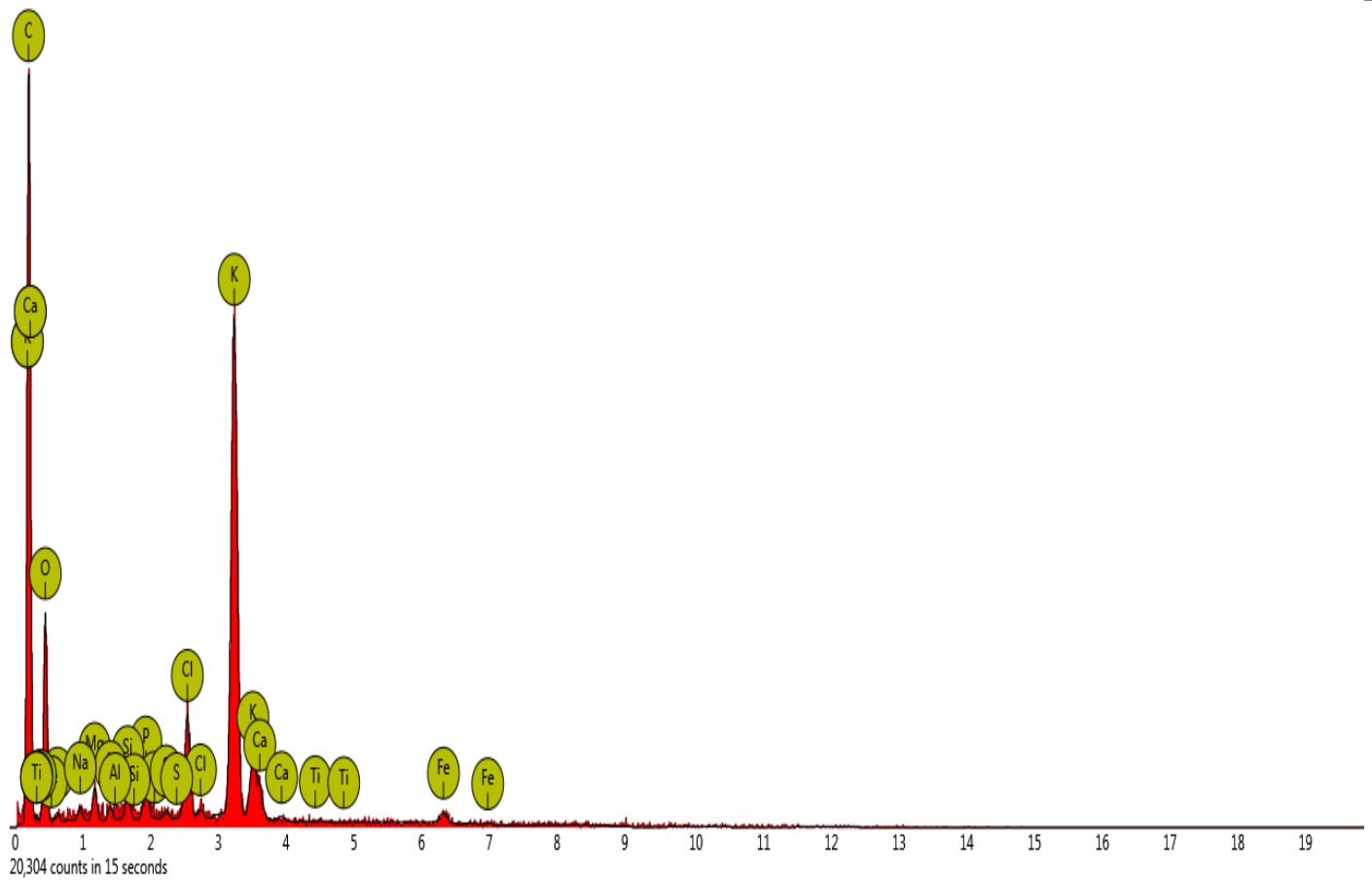
(F) Figure 1c (VI): Elemental analysis of Gros Michel Biochar
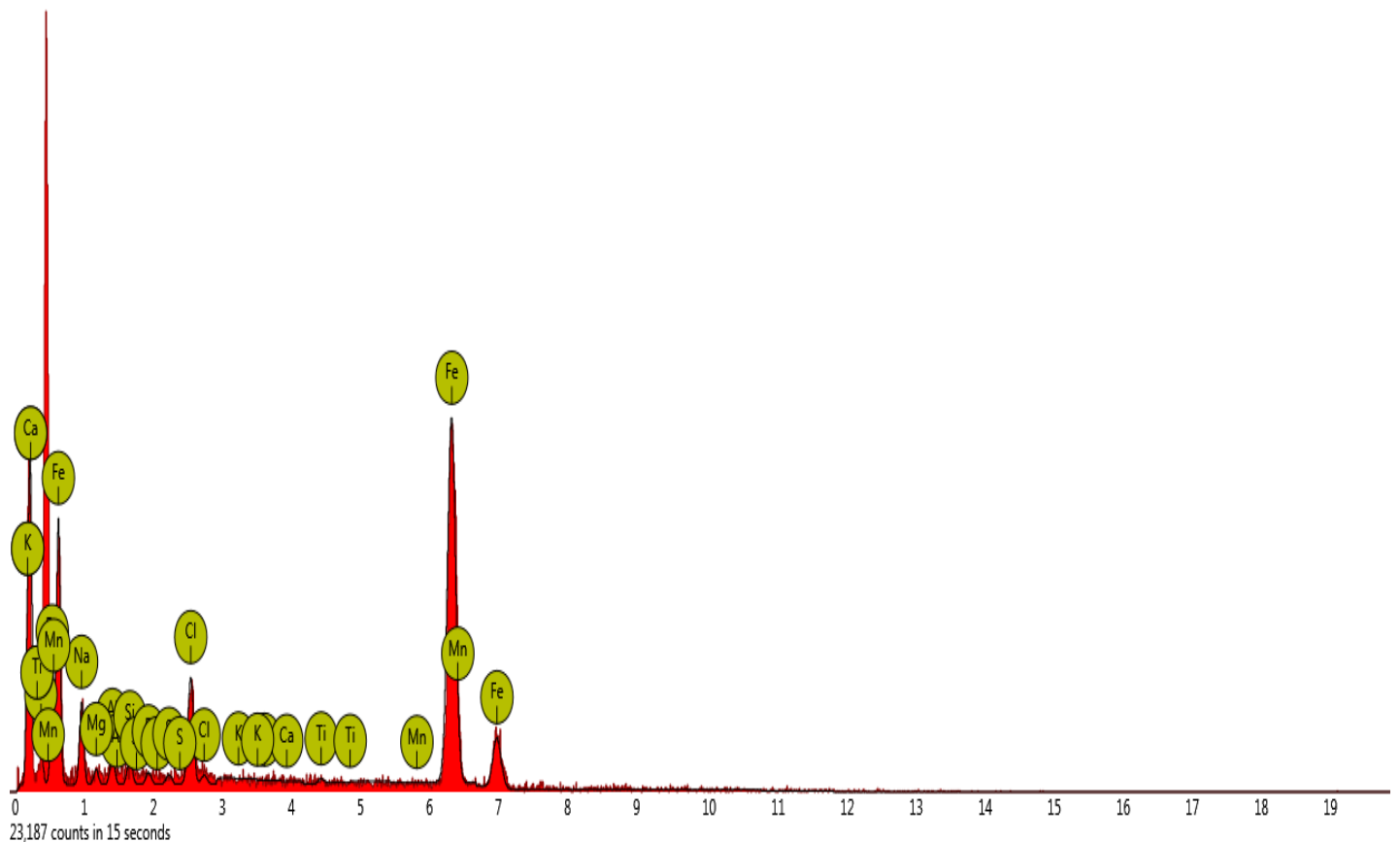
(G) Figure 1c (VII): Elemental analysis of F **Fe₃O₄**

23,610 counts in 15 seconds
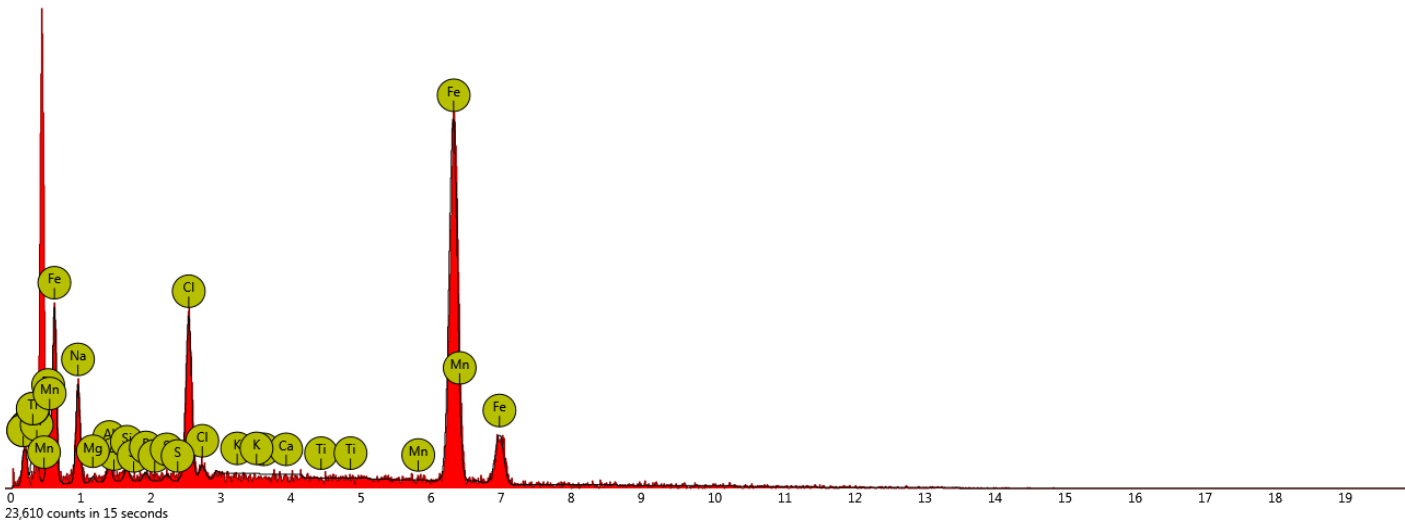
(H) Figure 1c (VIII): Elemental analysis of D Fe$_3$O$_4$

Table 2: Elemental Analysis of Adsorbents

	Element Number	Element Symbol	Element Name	Atomic Conc.	Weight Conc.
Cavendish Biochar	6	C	Carbon	80.47	62.29
	19	K	Potassium	9.80	24.70
	7	N	Nitrogen	6.37	5.75
	17	Cl	Chlorine	1.03	2.35
	20	Ca	Calcium	0.69	1.77
	15	P	Phosphorus	0.35	0.70
	12	Mg	Magnesium	0.41	0.64
	14	Si	Silicon	0.28	0.52
	26	Fe	Iron	0.11	0.41
	13	Al	Aluminium	0.21	0.37
	16	S	Sulfur	0.15	0.31
	11	Na	Sodium	0.13	0.19
	22	Ti	Titanium	0.00	0.00
Gros Michel Biochar	**6**	C	Carbon	63.20	48.04
	8	O	Oxygen	21.82	22.09
	19	K	Potassium	7.23	17.88
	7	N	Nitrogen	3.97	3.52

	17	Cl	Chlorine	1.20	2.69
	26	Fe	Iron	0.50	1.77
	20	Ca	Calci um	0.51	1.30
	15	P	Phosphorus	0.39	0.76
	12	Mg	Magnesium	0.42	0.65
	14	Si	Silicon	0.27	0.49
	11	Na	Sodium	0.25	0.37
	13	Al	Aluminium	0.15	0.25
	16	S	Sulfur	0.10	0.20
	22	Ti	Titanium	0.00	0.00
Fe₃O4 F	26	Fe	Iron	72.80	84.50
	11	Na	Sodium	13.16	6.29
	17	Cl	Chlorine	6.48	4.78
	13	Al	Aluminium	2.46	1.38
	14	Si	Silicon	1.85	1.08
	12	Mg	Magnesium	1.63	0.82
	15	P	Phosphorus	0.76	0.49
	16	S	Sulfur	0.58	0.39
	22	Ti	Titanium	0.28	0.28
	20	Ca	Calcium	0.00	0.00
	19	K	Potassium	0.00	0.00
	25	Mn	Manganese	0.00	0.00
Fe₃O4 D	26	Fe	Iron	70.71	82.92
	11	Na	Sodium	15.55	7.51
	17	Cl	Chlorine	9.65	7.19
	13	Al	Aluminium	1.62	0.92
	14	Si	Silicon	0.95	0.56
	15	P	Phosphorus	0.52	0.34
	12	Mg	Magnesium	0.59	0.30
	16	S	Sulfur	0.40	0.27

20	Ca	Calcium	0.00	0.00
19	K	Potassium	0.00	0.00
22	Ti	Titanium	0.00	0.00
25	Mn	Manganese	0.00	0.00

X-Ray Diffractometer Analysis (XRD)

XRD crystal structure of the synthesized adsorbents (Gros Michel Biochar, Cavendish Biochar, Fe_3O_4 D and Fe_3O4 F) are presented in figures 1d (I) – 1d (IV) and crystallite sizes of the adsorbents (D) in Table.3.
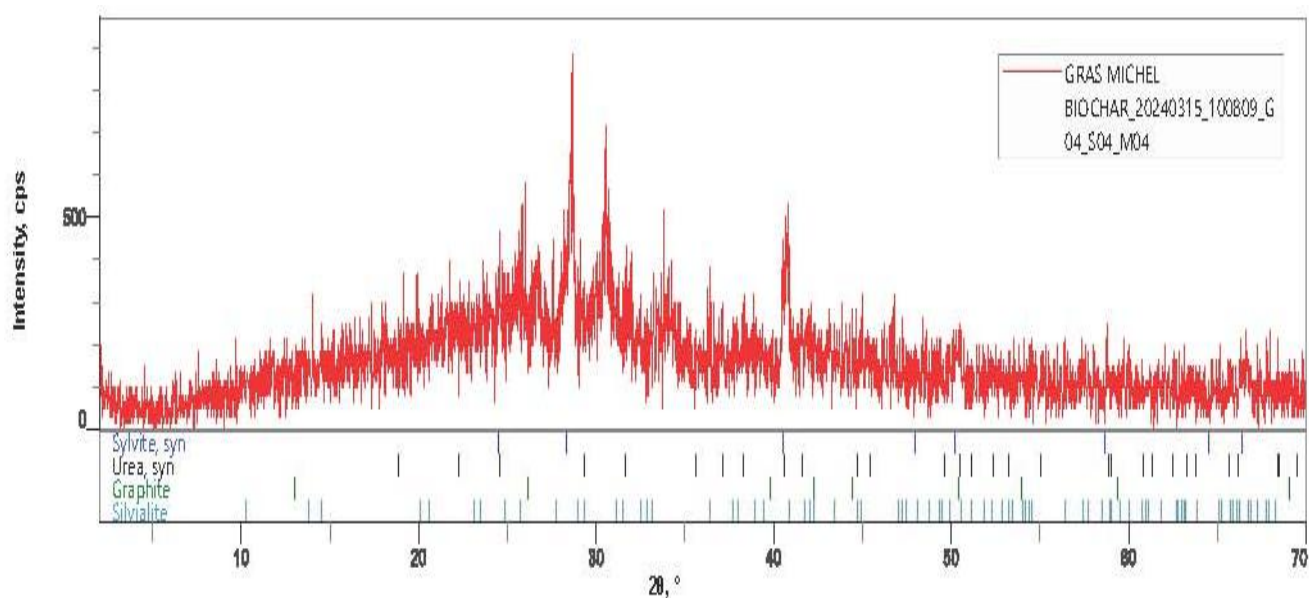

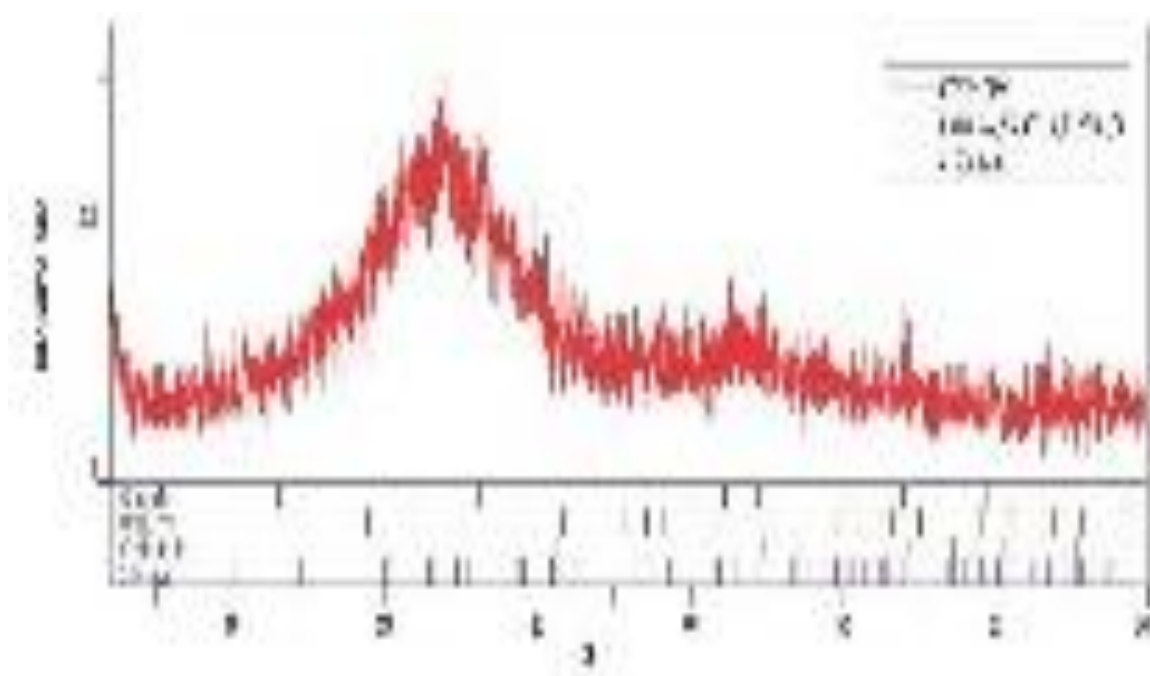**Figure 1d (I): XRD images of Gros Michel Biochar (A)**

Figure 1d (II): XRD images of Cavendish Biochar
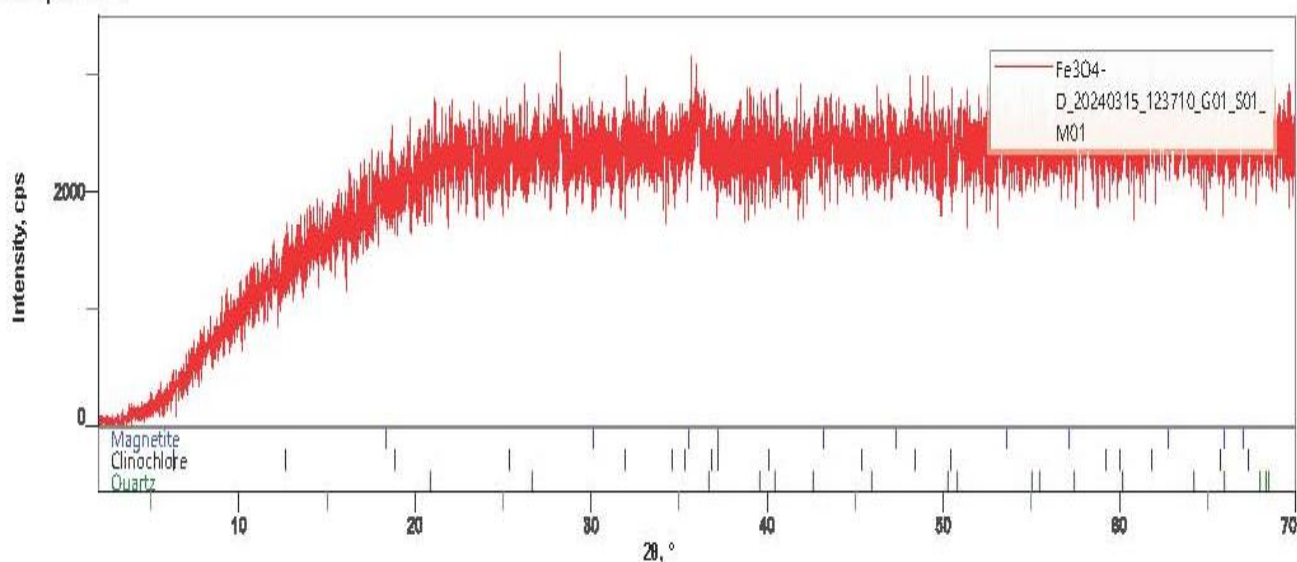
Figure 1d (III): XRD images of D Fe₃O₄
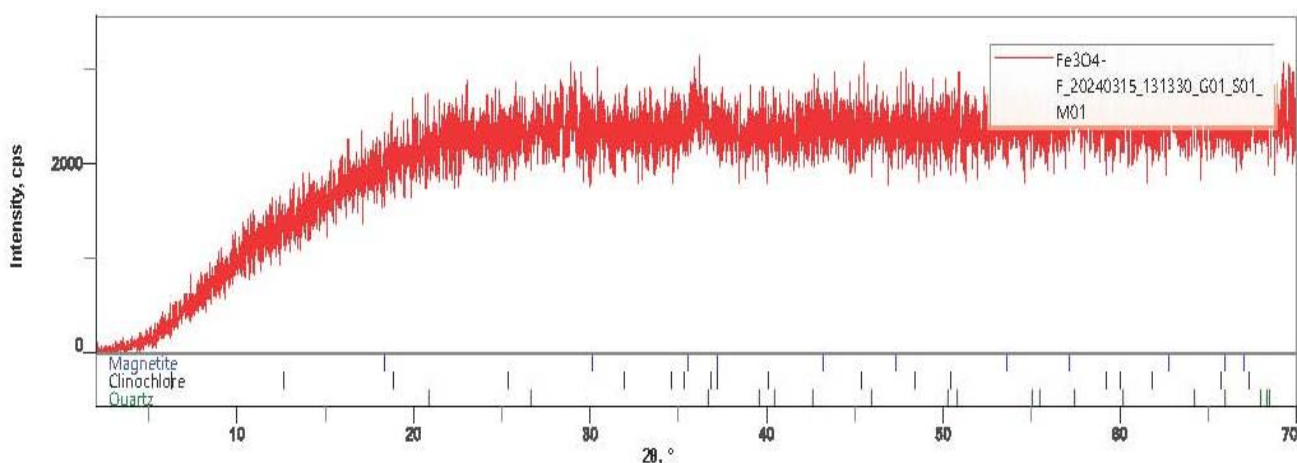
Figure 1d (IV): XRD images of F Fe₃O₄

Table 3: Calculation of the Synthesized Adsorbent Diameter from the XRD Spectra

Adsorbent	K	Θ	B	Λ	D (A⁰)
Gros Michel Biochar	0.94	13.26	2.7	1.947	1.442
Cavendish Biochar	0.94	23.3	14.4	2.52	0.35
D Fe₃O₄	0.94	17.8	52.3	2.93	0.112
F Fe₃O₄	0.94	15.2	44.2	3.359	0.152

DISCUSSION

Characterization of magnetite nanoparticle and biochar

FTIR

The FTIR spectrum of various synthesized adsorbents ranged from 701 cm^{-1} to 3131 cm^{-1} respectively as shown in figures 1a (I) - 1a (IV). Peaks and frequencies of IR absorption are presented in Table 1. The spectrum revealed

the presence of notable peaks like the O-H stretch present in all the adsorbent which can be attributed to the OH stretch in phenols present in the adsorbents. The peak located at around 1050 cm^{-1} in the various adsorbent can be ascribed to the C–O–H stretch. These functional groups are similar to the ones discovered by [12] and [13] and their presence enhance absorption. The reduction in -the peak intensity in the Fe nanoparticle spectra revealed that these groups may be involved in the process of nanoparticle synthesis. The C–Cl stretch due to alkyl halide at 753 cm^{-1} and NO$_2$ symmetric stretch due to nitro compound was observed only for the adsorbent prepared from the Cavendish biochar. According to [14] these adsorbents absorbed excellently.

TEM

TEM analysis was performed to understand the internal morphology of synthesized adsorbents (Gros Michel biochar, Cavendish Biochar, Fe$_3$O$_4$ D and Fe$_3$O4 F) at 50 nm. The micrographs for Gros Michel biochar and Cavendish biochar showed spherical morphology with slight agglomeration typical of particles prepared via a pyrolysis process shown in figures 1b (I) - 1b (II). The microgaphs of the iron oxide nanoparticles (figures 1b (III) and 1b (IV)) reviewed that the particles were agglomerated, spherical partial, cubic shape and have an amorphous structure as reported by [13], [15] and [16] with the inclusion of its properties aids absorption of pollutants. These results are compatible with X-ray and SEM analysis.

SEM and EDX

SEM is used to study the morphological characteristics such as size, shape and porosity of adsorbents. The scanning electron micrographs (figures 1c (I) - 1c (IV)) were taken to analyze the surface morphology of adsorbents Gros Michel, biochar, Cavendish Biochar, Fe$_3$O$_4$ D and Fe$_3$O$_4$ F at 10 μm. The micrograph of the surface of the prepared adsorbents showed the morphology of the surface adsorbent having pores, cracks, holes which are expected to enhance adsorption. In all cases, well-developed porous surface diameter in micrometer (μm) range. Were observed at higher magnification (2000 X). These pores are considered as channels to the micro porous network. The SEM images of the iron size nano particle (figure 3c and 3d) appeared as rode shape morphology and also are agglomerated. The magnetic -characteristics of iron particles should make it possible for iron oxide nanoparticles to exist in such close contact with each other, which matched with EDS and XRD data. The shape of the nanoparticles prepared by decantation differs from those prepared from filtration. This suggests that the type of the procedure used in the production of the nanoparticle has an effect on the shape and the size of the nanoparticles [17].

Also, a comparison of the micrographs presented in figures 1c (V) and 1c (VIII) revealed that the Fe$_3$O$_4$ D adsorbent which was prepared by decantation of the synthesized nano particle possses more pores, caves type openings, rough texture with heterogeneous surface and a variety of randomly distributed pore size and good surface area than the other three adsorbents. Hence this implies that the Fe$_3$O$_4$ D adsorbent is having good adsorptive ability than the other adsorbents.

The data generated by EDS consist of spectra showing peaks (figure 3e to 3h) corresponding to the elements making up the true composition of the sample being analyzed. The elements of adsorbents Gros Michel biochar, Canvendish biochar, Fe$_3$O$_4$ D and Fe$_3$O$_4$ F given in Table 2, which shows the Cavendish biochar has rich amount of carbon 80.47 % and traces of Potassium, Nitrogen , Chlorine, Calcium, Phosphorus, Magnesium, Silicon, Iron, Aluminium Sulphur, and Sodium, therefore purity is high.

X-Ray diffractometer analysis (XRD)

The crystal structure of the synthesized adsorbents (Gros Michel biochar, Cavendish biochar, Fe$_3$O$_4$ D and Fe$_3$O4 F) were determined using an X-ray diffraction (XRD) technique and the result obtained are presented in figures 1d (I) to 1d (IV). The XRD patterns obtained for Gros Michel biochar and Cavendish biochar (figures 1d (I) and 1d (II)) were similar to that of grahite while that obtained for Fe$_3$O$_4$ D and Fe$_3$O4 F (figures 4c and 4d) were similar with that reported by [18] for iron oxide nanoparticle. The peaks obtained were identified by comparing them with the Joint Committee on Powder Diffraction Standards (JCPDS) files [19]. Six distinct peaks at 2θ = 67°, 50°, 26°,29°, 31° and 41° with the phase plane of (220), (311), (400), (422), (511) and (440) respectively were obtained for the Gros Michel biochar adsorbent. However only one distinct peak at 47° was observed for

the Cavendish biochar adsorbent. These observed peaks denote the formation of a crystalline carbonaceous structure [20].

The XRD analysis of Fe_3O_4 D and Fe_3O4 F adsorbents shown in figures 1d (III) and 1d (IV) indicate that the synthesized Fe nanoparticles were amorphous with weak characteristic peak of iron, implying the non-crystalline nature of the iron nanoparticles. This weak diffraction peaks are consistent with the standard diffraction of Fe–O powders which confirm the formation of magnetite (JCPDS File No. 74–1886) [20].

The crystallite sizes were estimated using Scherrer's formula;

$$D = \frac{K\lambda}{\beta Cos\theta}$$ (I)

Where the D is the crystallite size, K is a constant taken to be 0.94, λ is the wavelength of X-ray, β is the half width of the most intense peak and θ is the Bragg angle of the most intense peak. Using this equation, the various crystallite sizes of the adsorbents were calculated and reported in Table 3.

The average particle size of Gros Michel biochar, Cavendish biochar, Fe_3O_4 D and Fe_3O4 F as calculated from equation 1 was found to be 1.442, 0.35, 0.112 and 0.152 A^o respectively 11 nm which confirmed that the synthesized nanoparticles were nano crystalline in nature

CONCLUSION

Magnetite nanoparticle and biochar from unripe banana peels were successfully produced. Their characterization revealed the presence of hydroxyl (OH) functional group, pores, cracks, holes, agglomerated, grahite pattern, nano crystalline in nature which enhanced absorption of pollutants.

REFERENCES

1. Samuel. O. B. & Omoleomeo, O. Omo-Irabor (2016). Environmental Impact Assessment of Selected Oil Production Facilities in Parts of Niger Delta, Nigeria. Journal of Water Resource and Protection, 8 (2), 237–42.
2. Ejiba, I. V. Onya, S. C. & Adams, O. K. (2016). Impact of oil pollution on livelihood: evidence from the Niger Delta region of Nigeria. Journal of Scientific Research and Reports, 1, 12.
3. Khan, I. A, Saeed, K. B. & Khan I. (2019). Nanoparticles: Properties, applications and toxicities. Arabian Journal of Chemistry, 12(3), 908-931.
4. Machado, S.; Pacheco, J. G., Nouws, H. P. A., Albergaria, J. T &. Delerue-Matos, C. (2015). Characterization of green zero-valent iron nanoparticles produced with tree leaf extracts. Science Total Environmental, 533, 76–81.
5. Nhuchhen, D., Basu, P. & Acharya, B. (2014). A comprehensive review on biomass torrefaction. International Journal of Renewable Energy and Biofuels, 1–56.
6. Alhashimi, H. A. & Aktas, C. B. (2017). Life cycle environmental and economic performance of biochar compared with activated carbon: A meta-analysis. Resources, Conservation and Recycling, 118, 13-26.
7. Joshua, O. I. & Adewale, G. A. (2020). Biomass to Biochar Conversion for Agricultural and Environmental Applications in Nigeria: Challenges, Peculiarities and Prospects. Materials International, 2(2), 111-116.
8. Akpomie, K. G. & Conradie, J. (2020). Synthesis, characterization, and regeneration of an inorganic–organic nanocomposite and its application in the capture of cationic dye. Scientific Reports. 10: 14441.
9. Khan, I. A, Saeed, K. B. & Khan I. (2019). Nanoparticles: Properties, applications and toxicities. Arabian Journal of Chemistry, 12(3), 908-931
10. Ebiana, C. A. &. Konne, J. L. (2016). Fenton-like degradation of polycyclic aromatic hydrocarbons (pahs) using starch stabilized magnetic nanoparticles (SSMNPS), and magnetite (MNPS-Fe_3O_4) Journal Chemical Society of Nigeria, 41(2), 39-45.
11. Yunqiang, W., Zhengkang, Z., Xinliang, S., Fengting, W., Ying, Z., Zhen, L., Licong, Y., Zhaoyi, D. & Junli, L. (2021). Physiologicalof biochar and a Fe_2O_3 nanoparticles as amendment of Cd accumulation

and toxicity toward muskmelon grown in pots. Journal of Nanobiotechnology, 19, 442.

12. Fawzia I. E-D, Dalia E. M., Omnia A.A. E-S., Marwa R. M. (2020). Study the adsorption properties of magnetite nanoparticles in the presence of different synthesized surfactants for heavy metal ions removal. Egyptian Journal of Petroleum, 29 (1), 1-7

13. Amlan, D., Avinash, M. & Ruchi, V. (2014). Bio-Reductive Synthesis and Characterization of Plant Protein Coated Magnetite Nanoparticles. Nano Hybrids, 7, 69-86

14. Ebuka, C. E., Joy, A., Kingsley O. I., Samuel, O., Comfort A. A., Victor, T. A., Hussein, K. O. & Adewale, G. A. (2022). Adsorption of crude oil from aqueous solution: Journal of Water Process Engineering, 50, 103330.

15. Asfaram, A., Ghaedi, M., Agarwal, S., Tyagi, I. & Gupta, V.K. (2015) Removal of basic dye Auramine-O by ZnS: Cu nanoparticles loaded on activated carbon: optimization of parameters using response surface methodology with central composite design, RSC Adv. 5 (24) (2015) 18438–18450.

16. Ighalo, J. O., Iwuozor, K. O., Igwegbe, C. A. & Adeniyi, A.G. (2021). Verification of pore size effect on aqueous-phase Adsorption kinetics: a case study of methylene blue, Colloid. Surface. Physicochemical Engineering. Aspect, 127119.

17. Ameh, P. O. (2022). Utilization of Nanoparticle Prepared from Local Nigerian Hen Egg Shell as an Adsorbent for the Removal of Methylene Blue dye from aqueous solution. Chemical Review and Letters journal, 5, 29-43. www.chemrevlett.co m ISSN (online): 2645-4947.

18. Dinali R, Ebrahiminezhad A, Manley-Harris M, Ghasemi Y, Berenjian A (2017). Iron oxide nanoparticles in modern microbiology and biotechnology. Critical Review Microbiology, 43(4), 493-507.

19. Ameh (2023). Synthesized ironoxide nanoparticles from Acacia noitica leaves for the sequestration of some heavy metal ions in aqueous solution. Journal of Chemical letters 4(1), 1-13.

20. Eddy,N. O., Garg,R., Ukpe, R. A., Ameh, P. O., Garg, R., Runde, M., KwanchiI. D., Wabaidur, S. M., Aftab, S., Ogbodo, R., Aikoye, A. O. & Siddiqu, M. (2024). Application of periwinkle shell for the synthesis of calcium oxide nanoparticles and in the remediation of Pb2+ -contaminated water, Biomass Conversion and Biorefinery, 1 – 19.